

International Journal of Scientific Research and Reviews

Removal of Cd (II) and Pb (II) from aqueous solution using Green synthesized iron oxide nanoparticles onto *Aristolochia bracteolata* L.

P. Ramesh¹ and T. Damodharam^{1*}

¹ Sri Venkateswara University, Department of Environmental Sciences, Tirupati, Andhra Pradesh, India. Email: thotidamodharam@yahoo.co.in

ABSTRACT

Green synthesized iron oxide nano sorbent was prepared using an aqueous extract of *Aristolochia bracteolata* leaf as reducing agent. The structural properties of the nano-adsorbent was characterized by XRD and SEM, FT-IR spectroscopy and desorption studies were analysis. XRD and SEM methods indicate that nanoparticles were crystalline, spherical, size ranges from 68-116 nm, with an average size of 38 nm. Batch experimental parameters like pH, contact time, adsorbent dosage and metal ion concentrations were studied. The maximum removal of Cd (II) was 94.1% at pH 6 and Pb (II) 96.6% at pH 5 with an initial metal ion concentration of 50 mg/L. The adsorption isotherm data fitted well to Langmuir isotherm model and the monolayer adsorption capacity values for Cd (II) was 90.90 and for Pb (II) was 83.33 mg/g at 303 K; it is a good adsorbent for removal of Cd (II) and Pb (II) ions from industrial waste waters and advantages like environmental friendly and reusability.

KEY WORDS: *Aristolochia bracteolata*, XRD, SEM, Iron oxide nanoparticles, Nano-adsorbent

***Corresponding author:**

T. Damodharam

Sri Venkateswara University,
Department of Environmental Sciences,
Tirupati, Andhra Pradesh, India.

Email: thotidamodharam@yahoo.co.in

1. INTRODUCTION

Heavy metal pollution has become one of the most serious environmental problems. The treatment of heavy metals is of special concern due to their recalcitrance and persistence in the environment¹. With the rapid development of industries such as fertilizer industries, tanneries, metal plating facilities, batteries, paper industries and pesticides, heavy metals wastewaters are directly or indirectly discharged into the environment increasingly, especially in developing countries². Heavy metals such as cadmium and lead are generated in milling, electroplating, electrolytic depositions, conversion coating, smelting and mining. They can be absorbed and accumulated in human body and caused serious health effects like cancer, hyperglycemia, immune deficiency, anemia, damage the kidney, liver and reproductive system, basic cellular processes and brain functions^{3,4} and more toxic effects on the aquatic environment⁵.

Removal of heavy metals from industrial waste water can be accomplished through various conventional technologies, including chemical precipitation^{6,7}, coagulation and flocculation⁸, reverse-osmosis⁹, ion-exchange¹⁰, membrane filtration^{11,12} and adsorption¹³. Among them, adsorption is one of the best methods for removal of heavy metals from waste water because it is easy to operate, inexpensive and high efficient¹⁴. Nano-sized iron oxide nanoparticles play an important role as efficient adsorbents because of their size, high surface and magnetic property^{15,16,17}. Till to date, considerable research attention has been paid to the removal of heavy metals from contaminated water via adsorption process.

Recently, green synthesis of iron oxide nanoparticles with different sizes and shapes has been reported using various plant extracts, such as green tea¹⁸, *Argemone mexicana* leaf extract¹⁹, *Tridax procumbens* leaf²⁰, Pineapple peel extract²¹, sorghum bran extracts²², *Colocasia esculenta* leaf extract²³, Rambutan peel waste extract²⁴, *Eucalyptus globulus* leaf extract²⁵, *Ocimum sanctum* leaf extract²⁶, watermelon rinds²⁷

Aristolochia bracteolata is belongs to the family Aristolochiaceae and known as worm killer. It has insecticidal properties. Its roots and leaves are bitter and antihelmintic, and are medicinally important. Almost every part of the plant has medicinal usage²⁸. The objectives of this study are: (i) synthesis of iron oxide nanoparticles using *Aristolochia bracteolata* leaf extract and their characterization with respect to XRD, FTIR and SEM (ii) the use of the synthesized nanoparticles as an the adsorbent for the removal of Cd (II) and Pb (II) from aqueous solution, and (iii) the analysis of the adsorption isotherm data using Langmuir and Freundlich models.

2. MATERIAL AND METHODS

2.1. Materials

FeCl₃·6H₂O, C₂H₃NaO₂, HCl were obtained from Sigma Aldrich, CdCl₂ and Pb (NO₃)₂ were purchased from Merck (India). Double distilled water used to prepare all the solutions.

2.2. Preparation of Leaf extract

Plant leaves were taken from the local fields of Tirupati, Andhra Pradesh, India. Leaves are thoroughly rinsed with double distilled water to remove the fine dust particles and later, the leaves are dried under shade at room temperature for 24 hours under dust free condition. Dried leaves are grinded with a mortar and pestle to make a powder. An amount of 10 g of leaf powder is mixed in to 100 ml double distilled water and refluxed for 1 h, at 80 °C until the colour of aqueous extract solution changes from watery to thick green. The resultant composition is cooled to room temperature and filtered with a Whatman No. 1 filter paper and the final extract is stored at 4 °C for further use.

2.3. Synthesis of iron oxide nanoparticles

Iron nanoparticles were prepared through an easy and eco-friendly method. The iron oxide nanoparticles were synthesized by a previously reported method²⁹ with slight modifications. 0.01 M Ferric chloride(0.1622gms) and 0.01 M sodium acetate(0.08203gms) was prepared by using distilled water. 10 mL of freshly prepared leaf extract was mixed to 10 mL of aqueous ferric chloride solution (0.01 ferrichloride + 0.01 M sodium acetate solution) with constant stirring for 1h at 60 °C, the resulting solution becomes homogenous black in color after 1h specify the formation of iron oxide nanoparticles. The nanoparticle solution was cooled to room temperature and the black product attained was isolated by applying an external magnetic field and washed with ethanol and dried in vacuum oven 90 °C for 12h and kept in a stoppard bottle for further use.

2.4. Instrumentations

Fourier transform-infrared (FT-IR) spectra of the *Aristolochia bracteolata* L plant leaf extract and the synthesized nanoparticles were recorded on a SHIMADZU 8400S. The crystalline structure of iron oxide nanoparticle was analyzed by powder X-ray diffraction pattern, recorded by SHIMADZU XRD-7000 which provides control modules for the complete range of diffractometer accessories together with the corresponding analysis software. XRD with Cu-K radiation in a θ -2 θ configuration ($\lambda = 1.540598$ Å). The size and morphology of the synthesized particles were determined from images recorded on a Hitachi S-3700N Scanning Electron Microscopic (SEM)

using an accelerating voltage of 300 kV. The metal ions concentrations were determined using atomic absorption spectrometer (AA 6300, Shimadzu, Japan).

2.5. Batch adsorption studies

The adsorption studies of Cd (II) and Pb (II) ions on green synthesized iron oxide nanoparticles were performed at room temperature. The stock solutions of Cd (II) and Pb (II) ions were prepared by dissolving an appropriate quantity of CdCl₂ and Pb(NO₃)₂ dissolving in double distilled water to give a volume of 100 ml. In all sets of experiments, fixed volume of metal solution in 50mL was stirred with desired nano-adsorbent dose (50 – 150 mg) for the period of two hours. Different conditions of pH (2 – 7), initial concentrations (50, 100, 150 mg/L) and contact time (30 – 180 minutes) were evaluated during the study. The first and final concentrations of the metal ions in the solution were measured using Atomic Absorption Spectroscopy. The amount of adsorbed heavy metal ions on the iron oxide nano-adsorbent in the equilibrium state was calculated using the following equation:

$$qe = \frac{(Ci - Ce)}{M} V \quad (1)$$

Where

qe (mg/g) is the equilibrium adsorption capacity of metal ions (Cd (II), Pb (II))

V is the volume of the solution; Ci and Ce are the initial and equilibrium concentrations (mg/L), respectively, of Cd (II) and Pb (II), and M is the adsorbent dosage (mg). Furthermore, the adsorption percentage was defined as follows:

$$Adsorption(\%) = \frac{(Ci - Ce)}{Ci} \times 100 \quad (2)$$

RESULTS AND DISCUSSIONS

2.6. Characterization

Fig. 2. Shows the XRD pattern of iron oxide nanoparticles using *Aristolochia bracteolata* leaf extracts. The results of X-ray diffraction (XRD) showed that the sample was iron oxide nanoparticles intense diffraction peaks indexed to (122) plane appearing at $2\theta = 34.5^\circ$ respectively. It indicates that the prepared iron oxide nanoparticles are cubic crystal structure³⁰. This result matches with JCPDS card number: 39v-1346. The crystallite size of the prepared sample was estimated using Debye – Scherrer formula:

$$L = \frac{K\lambda}{\beta \cos\theta} \quad (3)$$

Where β is the full-width half maxima (FWHM) in radians, λ is wave length of the X – ray Cu K-alpha $\lambda = 0.15418$ nm, θ is corresponding Bragg angle and K is the constant ($K = 0.94$) and the

estimated crystallite size is 13 nm.

The Fourier transform infrared (FTIR) spectroscopy measurements were carried out to identify the possible biomolecules responsible for capping and stabilization of nanoparticles. Fig.1. shows the FTIR spectrum of iron oxide nanoparticles shows the major absorption peaks at 3400, 2163, 1022 and 418 cm^{-1} . The broad absorption peak at 3300 cm^{-1} is corresponding to O-H stretching of alcohol and phenolic compounds. The band 2077 corresponds to the N-H / C-O stretching vibration. The band at 1631 cm^{-1} suggested the presence of amide group (N-H bending), raised by carbonyl stretch of proteins. The peaks at 1383 - 1022 cm^{-1} represents the characteristics of C-H bending vibration. The band at 418 cm^{-1} indicated the Fe-O stretching of iron oxide nanoparticles as reported earlier^{31, 32}. The band 418 cm^{-1} indicated the Fe-O stretching of Fe_2O_3 nanoparticles.

SEM has been a primary tool for examine the morphology of the nanoparticles. The SEM images Fig.3. Shows the synthesized nanoparticles 38nm with grain size ranging from 60-127 nm and are spherical in shape.

Adsorption studies

2.7. Effect of pH

The synthesized iron oxide nanoparticles can be used for the removal of heavy metal ions like Cd(II) and Pb(II) from water. pH is an important parameter that influences the adsorption process by way of modifying the functional groups of biomass. The effect of pH on the removal of Cd (II) and Pb (II) ions was conducted in the pH range of 2 to 7 at 303 K and was investigated by nano-adsorbent. As shown in Fig 4 (a) and (b) the percentage removal of metal ions Cd(II) and Pb (II) increased with increase in pH from 2 to 6 and above that pH the percentage removal decreased with an increase in pH. Maximum removal of Cd (II) 94.5%, at pH 6 and Pb (II) 95.6 %, at pH 5 with an initial metal ion concentration of 50 mg/L respectively. Decrease in metal ion removal at higher pH may be because of the formation of hydroxyl ions of metals³³. Similar trends have been reported in the removal of Cd (II)³⁴ and the removal of Pb(II)^{35,36}.

2.8. Effect of adsorbent dose

The adsorption efficiency of Cd (II) and Pb(II) was studied by varying the amount of adsorbent dosage from 0.2 to 0.6 g keeping other parameters (pH, and contact time) constant. The result shows that maximum percent removal of Cd (II) and Pb (II) was about 94.1 % and 96.6 % at the dosage of 0.5 g and initial concentration 50 mg/L (Fig 5 a and b). When adsorbent dose was increased from 50 to 150 % w/v then it decreases again after the dose increases from 50 to 150 mg/L

this effect may be due to the fact that some adsorption sites remain unsaturated during the batch adsorption process³⁷.

2.9. Effect of contact time

Metal ions removal percentage was increased with an increase in contact time. All parameters such as dose of adsorbent and pH of solution were kept constant. The results indicated that Cd (II) and Pb (II) removal were increased from 53.2 to 94.1% and 58.0 to 96.6 % with the contact time variation from 30 to 120 minutes respectively. Thus the results illustrate that the optimum contact time for maximum removal of Cd (II) 94.1%, and Pb (II) 96.6 % is 120 minutes as shown in Fig. 6. This result is important because equilibrium time is one of the important parameters for an economical wastewater treatment system. The short equilibrium time was in agreement with that reported by other researchers for the adsorption of other metal ions onto iron oxide nanoparticles^{38,39}

2.10. Adsorption isotherms

To evaluate the maximum adsorption capacity of nano-adsorbent and the equilibrium adsorption of Cd (II) and Pb (II) onto green synthesized iron oxide nano-adsorbent, the adsorption data were analyzed by the Langmuir and Freundlich isotherm models.

The Langmuir equation can be expressed by the linearized form:

$$\frac{C_e}{q_e} = \frac{C_e}{q_m} + \frac{1}{q_m b} \quad (4)$$

Where q_e is the equilibrium adsorption capacity of metal ion concentration onto the adsorbent (mg/g), C_e is the equilibrium metal ion concentration in the solution (mg/L), q_m is the maximum capacity of adsorbent (mg/g) and b (L/mg) is the equilibrium constant relating to the sorption energy. The values of the Langmuir constants (K_L , Q_{max}) and Freundlich constants (K , n) are presented for the adsorption of metal ions like cadmium (II), and lead (II) was shown in Table 1. It shows that the R^2 value for Langmuir isotherms is high than Freundlich isotherm R^2 of 0.999 whereas for cadmium (II), and 0.999 for lead (II). Fig. 8(a) and (b) shows that R^2 values for Freundlich isotherm model was found R^2 of 0.963 for cadmium (II) and 0.988 for lead (II). Fig. 7 (a) and (b) show that the experimental data fits the Langmuir adsorption isotherm well with maximum adsorption capacity of 90.90 and 83.33 mg/g for Cd(II) and Pb(II) respectively. The Freundlich isotherm is applicable for modeling the adsorption of metal ions on heterogeneous surfaces and the linearized form of isotherm is expressed as:

$$\log q_e = \log k_f + \frac{1}{n} \log C_e \quad (5)$$

Where K_f (mg/g) and “ n ” are the Freundlich isotherm constant that represents the adsorption

and the intensity of adsorbents, Fig. 8 (a) and (b) show the linear plot of Freundlich isotherms of Cd (II) and Pb(II) onto green synthesized nano-adsorbent at 303 K. The fitted constants for the Freundlich isotherm model, K_f , “n” and correlation coefficient (R^2) are calculated from the intercept and slope of the plot and are presented in Table 1. The values of $n > 1$ represent favorable adsorption condition⁴⁰ and the “n” values for Cd(II) is 5.617 and for Pb (II) is 7.042. These values suggest that green synthesized nano-adsorbent is a good adsorbent for the adsorption of Cd (II) and Pb (II) ions.

2.10. Desorption studies

Desorption studies are essential for regeneration and reuse of an adsorbent. For the desorption experiments, the recycling efficiency of the green synthesized iron oxide nanoparticles using *Aristolochia bracteolata* plant leaf extract, was investigated. From the pH study, the adsorption percentage for Cd (II) and Pb(II) was lower at lower pH. Hence, the acidic medium is expected to be a feasible approach for the regeneration of Cd (II) and Pb (II) loaded green synthesized iron oxide nanoparticles. Thus, dilute 0.1 N HCl solutions of different pH were used to study the desorption of metal ions from nano-adsorbent and results are presented in Fig.9. It was found that the desorption percentage values were 95.52, 86.70, 80.46 and 75.68% with HCl solutions of pH 1.5, 2.0, 3.0 and 4.0, respectively. At lower pH, higher desorption was observed because of the sufficiently high hydrogen ion concentration, which led to the strong competitive adsorption. The results indicate that iron oxide nanoparticles can be reused for removal of Cd (II) and Pb (II).

3. CONCLUSION

Adsorption of Cd (II) and Pb (II) from aqueous solution was studied by green synthesized iron oxide nanoparticles utilizing *Aristolochia bracteolata* leaf extract. The iron oxide nanoparticles were characterized by FTIR, SEM and XRD techniques. The synthesized nanoparticles were 38 nm with spherical in shape and grain size ranging from 60-127 nm. The operational parameters like pH, effect of nanosorbent dosage and contact time highly affect the overall Cd (II) and Pb (II) uptake of nanosorbent, pH have significant effect on the removal efficiency. The optimum time was observed to be 2 hours with optimum dosage was 0.5 g. Equilibrium models like Langmuir and Freundlich isotherm models were used for the study and equilibrium data. Adsorption of both metals has reached equilibrium after about (120 minutes). The maximum adsorption of Cd(II) and Pb(II) onto Green synthesized iron oxide nano-adsorbent was observed at pH 6 for Cd (II) and pH 5 for Pb (II) with maximum adsorption capacity values of 90.90 for Cd (II) and 83.33 mg/g for Pb(II) at 303 K. Desorption studies with 0.1N HCl revealed that iron oxide can be regenerated by treatment with HCl and can be reused as the nano-adsorbent for several cycles. The outcomes demonstrated that the

proposed nano-adsorption strategy is reasonable for the expulsion of cadmium and lead in industrial waste water.

ACKNOWLEDGEMENTS

This research did not receive any specific grant from funding agencies in the public, commercial, or not-for-profit sectors. The authors are thankful to College of Technology, Osmania University, Hyderabad, India for providing instrument facility.

REFERENCES:

1. Fu F, Wang Q. Removal of heavy metal ions from wastewaters: a review. *J Environ Manage*, 2011,92: 407- 418.
2. N.K. Srivastava and CB. Majumder. Novel biofiltration methods for the treatment of heavy metals from industrial wastewater. *J Hazard Mater*, 2008, 151: 1-8.
3. International Programme on Chemical Safety (IPCS). Cadmium. Poisons Information Monograph. PIM 089. <http://www.inchem.org/documents/pims/chemical/cadmium.htm>.
4. R. Naseem and S.S. Tahir. Removal of Pb (III) from aqueous solutions by using bentonite as an adsorbent. *Water Res.*2001, 35, 3982-3986.
5. W.A. David and P. Welbourn. Environmental Toxicology. Cambridge University Press, Cambridge, U.K, 2002
6. NK. Swamy, P. Singh and PI. Sarethy PI. Precipitation of phenols from paper industry wastewater using ferric chloride. *Rasayan Chem J*, 2011, 4: 452-456.
7. MJ Gonzalez-Munoz, MA Rodriguez, S Luquea and JR Álvarez. Recovery of heavy metals from metal industry wastewaters by chemical precipitation and nanofiltration. *Desalination*. 2006, 200: 742-744.
8. E. Lopez-Maldonado, M.T. Oropeza-Guzman, J.L. Jurado-Baizaval and A. Ochoa-Teran, Coagulation– flocculation mechanisms in wastewater treatment plants through zeta potential measurements. *Journal of hazardous materials*. 2014, 279, 1-10
9. L.F. Greenlee, D.F. Lawler, B.D. Freeman, B. Marrot and P. Moulin. Reverse osmosis desalination: Water sources, technology, and today’s challenges, *Water Res.* 2009, 43, 2317–2348.
10. B. Alyuz and S. Veli. Kinetics and equilibrium studies for the removal of nickel and zinc from aqueous solutions by ion exchange resins. *J Hazard Mater*. 2009, 167: 482-488.
11. J Landaburu-Aguirre, V Garcia, E Pongracz and RL Keiski. The removal of zinc from synthetic wastewaters by micellar-enhanced ultra filtration: statistical design of experiments. *Desalination*.

2009, 240: 262-269.

12. J Landaburu-Aguirre, E Pongracz, P Peramaki and RL Keiski. Micellarenhanced ultra filtration for the removal of cadmium and zinc: Use of response surface methodology to improve understanding of process performance and optimization. *J Hazard Mater.* 2010, 180: 524-534.
13. A. Tripathi and MR. Ranjan . Heavy metal removal from wastewater using low cost adsorbents. *J. Bioremed. Biodeg.* 2015, 6, 1-5.
14. MH Ehrampoush, H Masoudi, AH Mahvi and MH Salmani. Prevalent kinetic model for Cd (II) adsorption from aqueous solution on barley straw Fresenius. *Environ Bulletin.* 2013, 22(8):2314–8.
15. PN Dave and L.V. Chopda. Application of Iron Oxide Nanomaterials for the Removal of Heavy Metals. *Journal of Nanotechnology.* 2014, p. 1-14.
16. P Xu, GM Zeng, DL Huang, CL Feng, S Hu and MH Zhao. Use of iron oxide nanomaterials in wastewater treatment: a review. *Sci Total Environment.* 2012, 424:1–10.
17. J Gong, X Wang, X Shao, S Yuan, C Yang and X Hu. Adsorption of heavy metal ions by hierarchically structured magnetite-carbonaceous spheres. *Talanta.* 2012, 101:45–52.
18. T. Shahwan, S. Abu Sirriah, M. Nairat, E. Boyac, A.E. Eroglu, T.B. Scott, K.R. Hallamc (2011). Green synthesis of iron nanoparticles and their application as a Fenton-like catalyst for the degradation of aqueous cationic and anionic dyes. *Chemical Engineering Journa.* 2011, 172; 258– 266.
19. S. Arokiyaraj, M. Saravanan, N.K. Udaya Prakash, M. Valan Arasu, B. Vijayakumar, S. Vincent . Enhanced antibacterial activity of iron oxide magnetic nanoparticles treated with *Argemone mexicana* L. leaf extract: An in vitro study. *Materials Research Bulletin.* 2013, 4; 3323–3327.
20. Sneha Shah, Sumita Dasgupta, Mousumi Chakraborty, Raji Vadakkekara, Murtaza Hajoori. Green synthesis of iron nanoparticles using plant extracts. *International Journal of Biological & Pharmaceutical Research,* 2014. 5(6): 549-552.
21. S. Venkateswarlu, Y.S. Rao, T. Balaji, B. Prathima and N.V.V. Jyothi. Biogenic synthesis of Fe₃O₄ magnetic nanoparticles using plantain peel extract. *Mat. Lett.* 2013, 100, 241–244.
22. E.C. Njagi, H. Huang, L. Stafford, H. Genuino, HM. Galindo, J.B. Collins, GE. Hoag and S.L Suib. Biosynthesis of iron and silver nanoparticles at room temperature using aqueous sorghum bran extracts. *Langmuir.* 2011, 27, 264–271.
23. S. Thakur and N. Karak. One-step approach to prepare magnetic iron oxide/reduced graphene oxide nanohybrid for efficient organic and inorganic pollutants removal. *Materials Chemistry and Physics.* 2014, vol. 144, no. 3, pp. 425–432.

24. R. Yuvakkumar and S.I. Hong. Green Synthesis of Spinel Magnetite Iron Oxide Nanoparticles, *Advanced Materials Research*. 2014, Vol. 1051; pp 39-42
25. Z. Wang. Iron complex nanoparticles synthesized by eucalyptus leaves. *ACS Susta. Chem. Eng.* 2013, 1, 1551–1554.
26. M.G. Balamurugan, S. Mohanraj, S. Kodhaiyoli and V. Pugalenth. Ocimum sanctum leaf extract mediated green synthesis of iron oxide nanoparticles: spectroscopic and microscopic studies. *J. Chem. Pharmaceu. Sci.* 2014, 4, 201-204.
27. CH Prasad, S Gangadhara and P. Venkateswarlu. Bio-inspired green synthesis of Fe₃O₄ magnetic nanoparticles using watermelon rinds and their catalytic activity, *Appl. Nanosci.* 2016, 6, 797–802.
28. D. Kavitha and R. Nirmaladevi. Assessment of Aristolochia bracteolata leaf extracts for its biotherapeutic potential. *African Journal of Biotechnology*, 2009, Vol. 8 (17), pp. 4242-4244.
29. Sada Venkateswarlu and M.Yoon. Rapid removal of cadmium ions using green synthesized Fe₃O₄ nanoparticles capped with diethyl-4-(4 amino-5-mercapto-4H-1, 2, 4-triazol-3-yl) phenyl phosphonate. *RSC Adv.* 2015, 5, 65444–65453.
30. Mona Mahmoud Abd El-Latif, Amal M. Ibrahim, Marwa S. Showman, Rania R. Abdel Hamide. Alumina/Iron Oxide Nano Composite for Cadmium Ions Removal from Aqueous Solutions, *International Journal of Nonferrous Metallurgy*, 2013, 2, 47-62.
31. H.R. Wang and K.M Chen. Preparation and surface active properties of biodegradable dextrin derivative surfactants biodegradable dextrin derivative surfactants. *Colloids and Surfaces A: Physicochem. Eng. Aspects.* 2006, 281, 190 -193
32. N Latha and M Gowri. Bio synthesis and characterization of Fe₃O₄ nanoparticles using Caricaya papaya leaves extract. *Inter. J. Sci. Res.* 2014, 3, 1551-1556
33. B Sreenu, S Priti, K Seshaiyah and A.P Singh. Synthesis and characterization of nanoporous silica SBA-15 diaminocyclohexane and its application in removal of Cu (II) and Ni (II) from aqueous solution. *Desali. Water Treat.* 2016, 57, 15397–15409.
34. D. S. Shirsath B. N. Patil V. S. Shirivastava. Rapid removal of metals from aqueous solution by magnetic nanoadsorbent: A kinetic study. *Int. J.Nano Dimens.* 2013, 3(4): 303-312.
35. HZ Mousavi, A. Hosseynifar, V. Jahed and S.A.M Dehghani. Removal of Lead from Aqueous Solution Using Waste Tire Rubber Ash as an Adsorbent, *Brazilian Journal of Chemical Engineering, Brazilian Journal of Chemical Engineering.* 2010, Vol. 27, No. 01, pp. 79 – 87.
36. Nashaat N. Nassar. Kinetics, Equilibrium and Thermodynamic Studies on the Adsorptive Removal of Nickel, Cadmium and Cobalt from Wastewater by Super paramagnetic Iron Oxide Nanoadsorbents, *Can. J. Chem. Eng.* 2012, 90:1231–1238.

37. K Hardiljeet, Boparai & Meera Joseph and M Denis. Cadmium (Cd²⁺) removal by nano zerovalent iron: surface analysis, effects of solution chemistry and surface complexation modeling. *Environ Sci Pollut Res.* 2013, 20:6210–6221.
38. H Sun, X Zhang, Q Niu, Y Chen and J.C Crittenden (2007). Enhanced accumulation of arsenate in carp in the presence of titanium dioxide nanoparticles. *Water, Air, and Soil Pollution.* 2007, vol. 178, no. 1–4, pp. 245–254.
39. Rais Ahmad and Rajeev Kumar (2010). Adsorption studies of hazardous malachite green onto treated ginger waste, *Journal of Environmental Management.* 2010, 91, 1032–1038.
40. Uzaira Rafique, Anum Imtiaz, Abida K. Khan. Synthesis, Characterization and Application of Nonmaterial's for the Removal of Emerging Pollutants from Industrial Waste Water, Kinetics and Equilibrium Model. *Journal of Water Sustainability.* 2012, Volume 2, Issue 4, 233–244.

Table 1. Langmuir and Freundlich isotherm constants for Cd (II) & Pb (II) by Green synthesized (*Aristolochia bractelata* L.) iron oxide nanoparticles.

Metal ions	Langmuir			Freundlich		
	qm(mg/g)	b(L/mg)	R ²	Kf(mg/g)	n	R ²
Cd(II)	90.90	0.366	0.999	39.62	5.617	0.963
Pb(II)	83.33	0.50	0.999	44.15	7.042	0.988

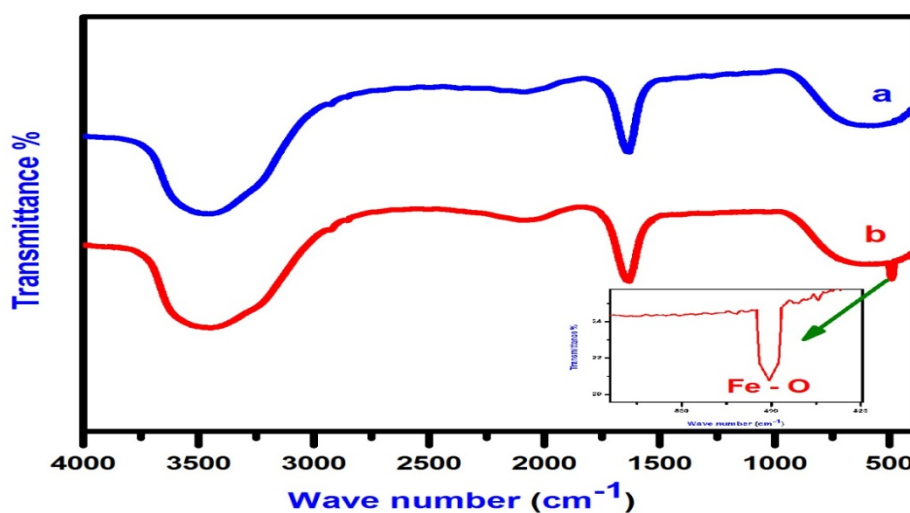


Fig. 1 FTIR spectra of green synthesized iron oxide nanoparticles

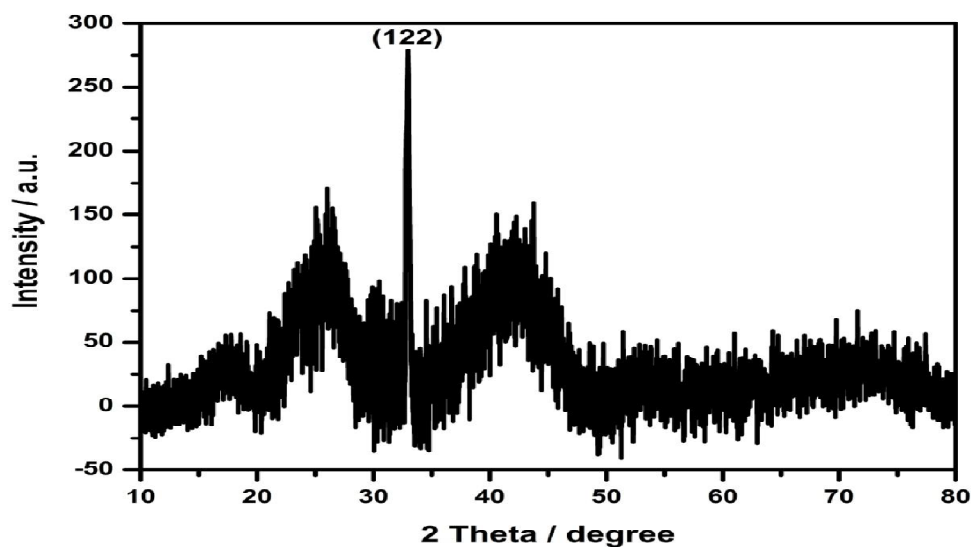


Fig. 2 XRD images of synthesized iron nanoparticles

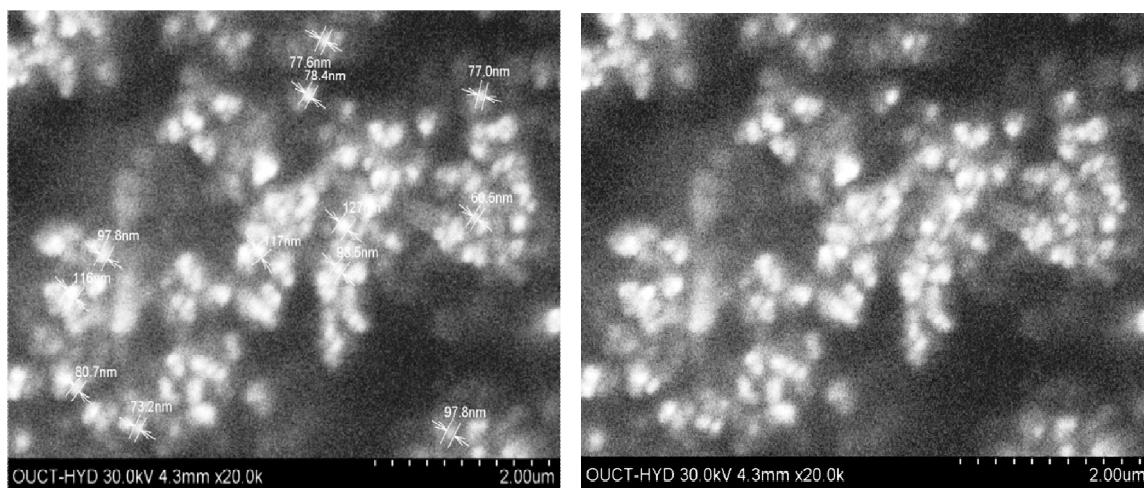


Fig. 3 SEM of synthesized iron oxide nanoparticles from leaf extract

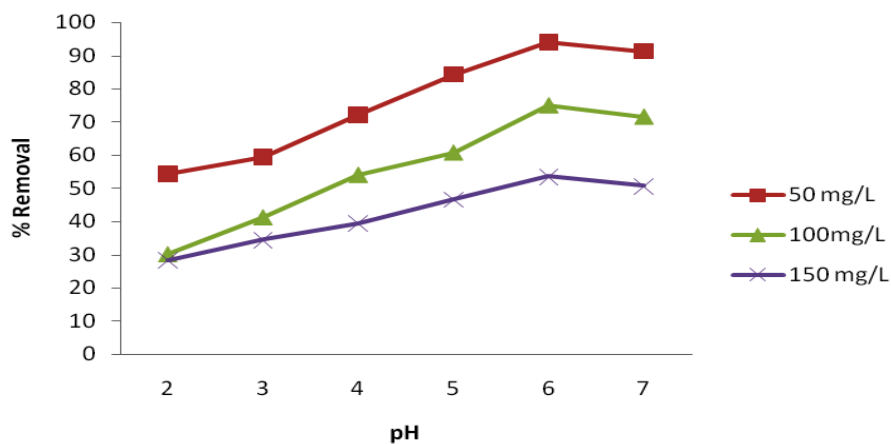


Fig. 4(a) Effect of varying pH on metal ion Cd(II) adsorption by nano-adsorbent at different initial concentrations ((initial concentrations of Cd(II) 50, 100, 150 mg/L, material dosage:0.5 g/L, solution volume: 50 mL, time: 120 min, temperature: 303 K).

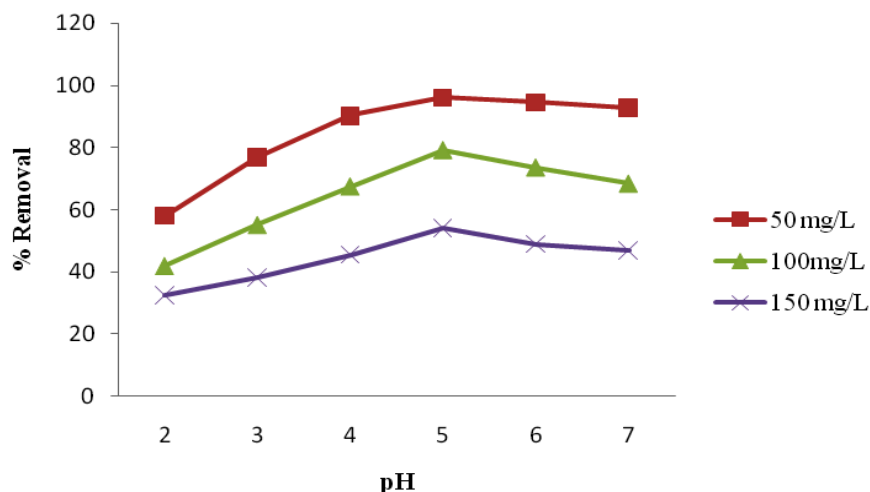


Fig.4(b) Effect of varying pH on metal ion Pb(II) adsorption by nano-adsorbent at different initial concentrations ((initial concentrations of Pb(II) 50, 100, 150 mg/L, material dosage: 0.5 g/L, solution volume: 50 m/L, time: 120 min, temperature: 303 K).

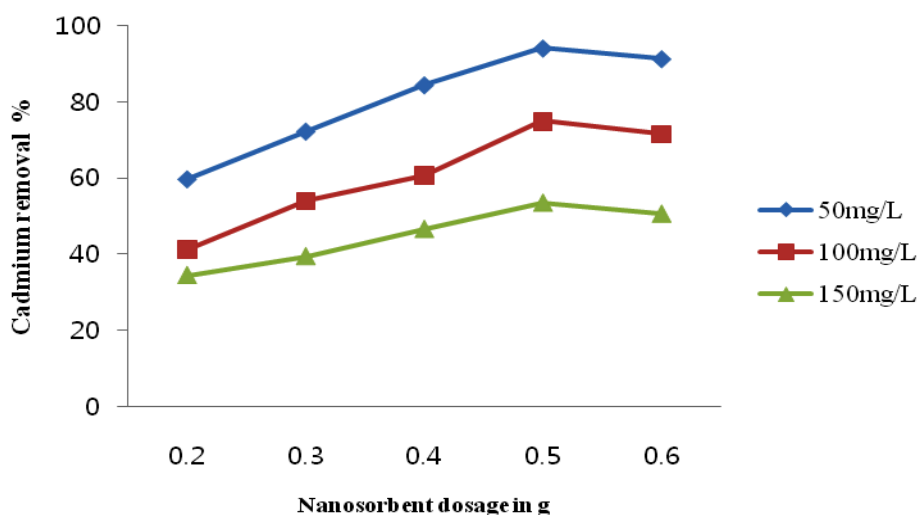


Fig. 5(a) Effect of nano-adsorbent (g) on the percentage removal of Cadmium at pH=6 and different initial concentrations (initial concentrations: 50, 100, 150 mg/L, material dosage: 0.5 g/L, solution volume: 50 m/L, time: 120 min, temperature: 303 K).

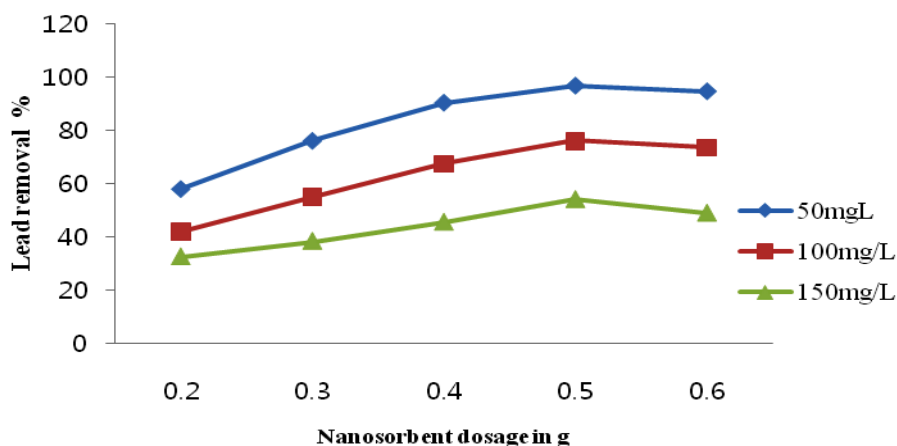


Fig. 5(b) Effect of nanosorbent (g) on the percentage removal of Lead at pH=5 and different initial concentrations (initial concentrations: 50, 100, 150 mg/L, material dosage: 0.5 g/L, solution volume: 50 mL, time: 120 min, temperature: 303 K).

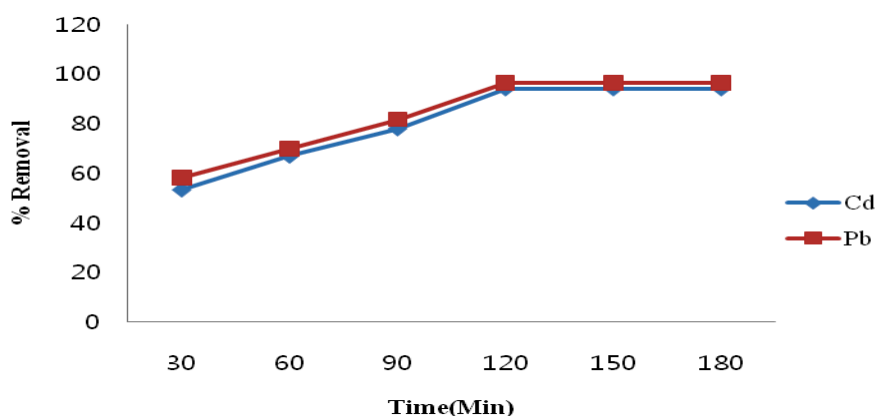


Fig. 6. The effect of contact time on the Cd (II) and Pb(II) removal efficiency at pH=6 and initial concentration 50 mg/L.

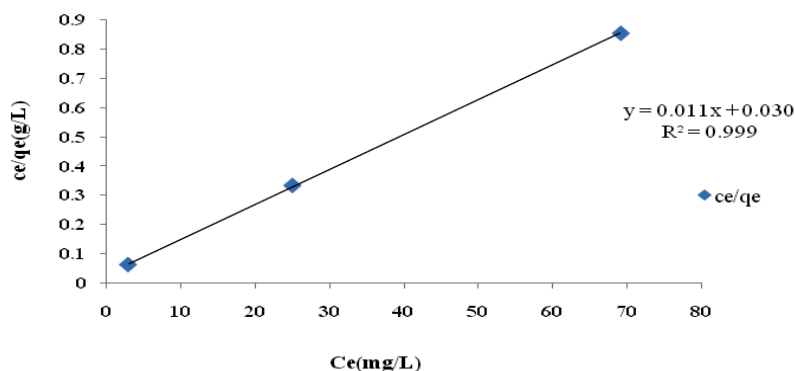


Fig.7(a) Linear plot of Langmuir isotherm of Cd (II) onto green synthesized iron nano-adsorbent

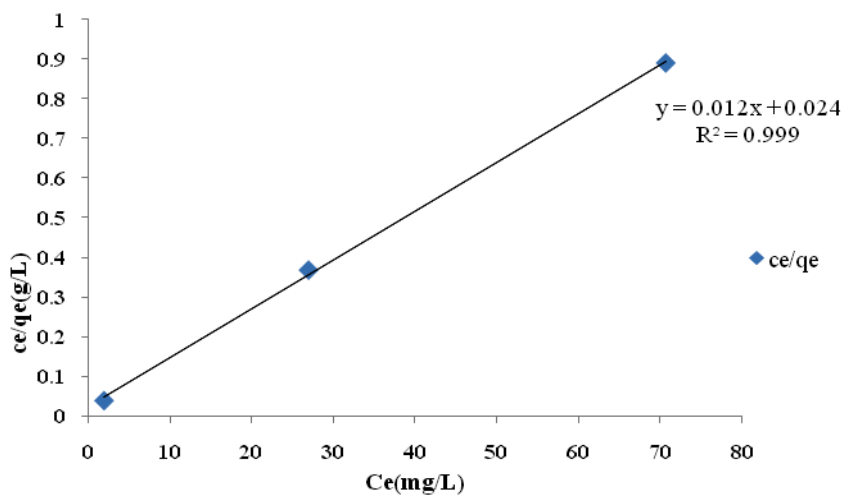


Fig. 7(b) Linear plot of Langmuir isotherm of Pb (II) onto green synthesized iron nano-adsorbent

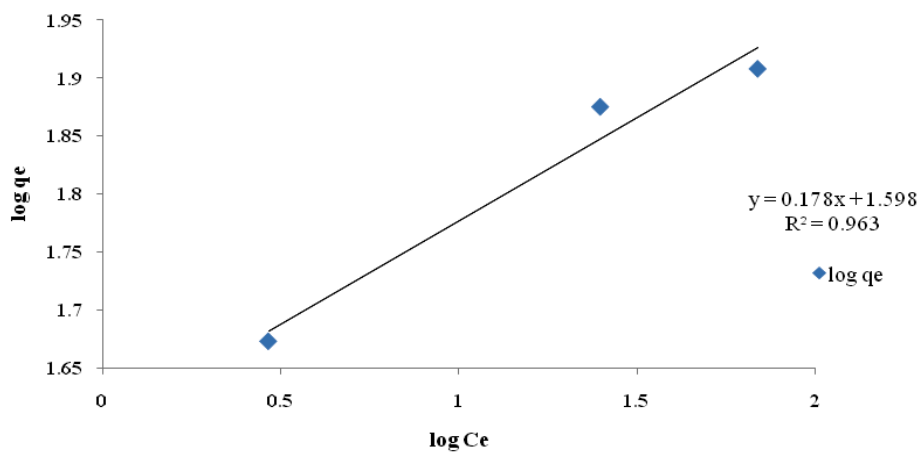


Fig.8(a) Linear plot of Freundlich isotherm of Cd (II) onto green synthesized iron nano- adsorbent

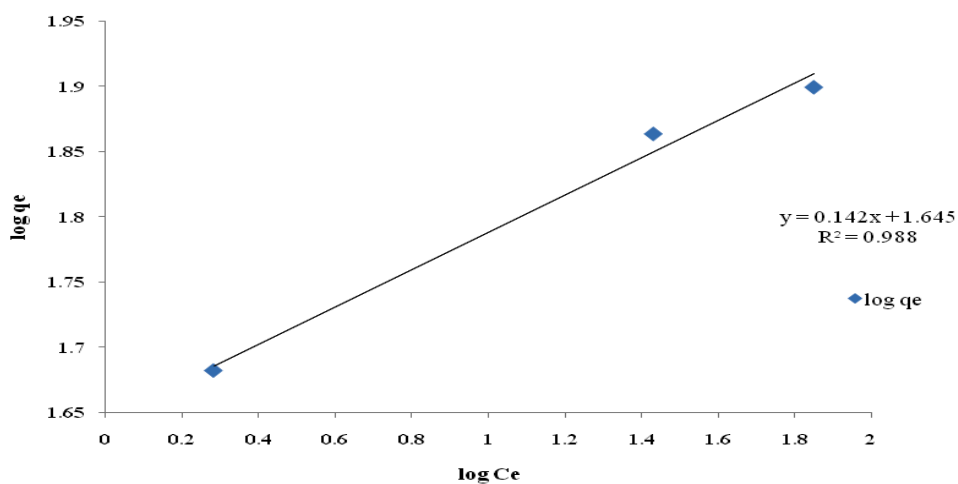


Fig. 8(b) Linear plot of Freundlich isotherm of Pb (II) onto green synthesized iron nano-adsorbent

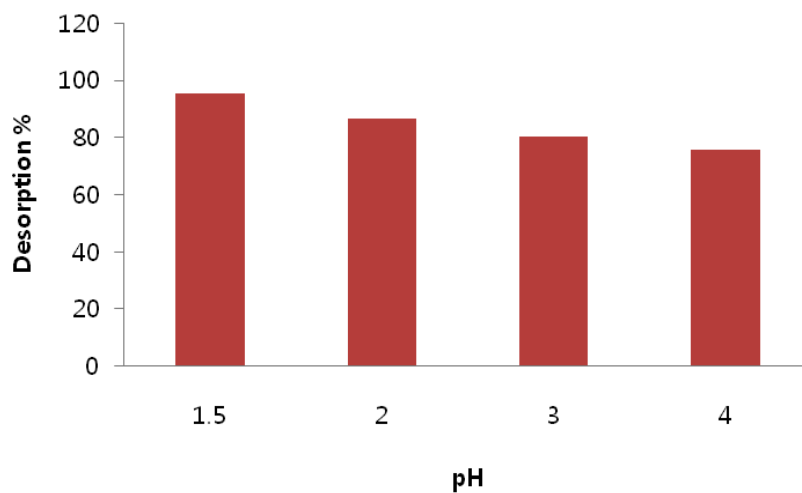


Fig. 9 Desorption efficiency of Cd(II) and Pb(II) with 0.1N HCl at different pH